Histopathological and immunofluorescent characterization of post-sepsis immune dysregulation in a clinically relevant mouse model

Haoran Tang,[1]* Chen Liao,[1]* Ning Tang,[2] Hui Li,[3] Yi Liu,[3] Lingling Wang,[4] Zongfang Ren[3]

[1]Department of Gastroenterological Surgery, the Second Affiliated Hospital of Kunming Medical University, Kunming, Yunnan
[2]Department of Neurology, the First People's Hospital of Yunnan Province, Kunming University of Science and Technology, Kunming, Yunnan
[3]Department of Critical Care Medicine, the Second Affiliated Hospital of Kunming Medical University, Kunming, Yunnan
[4]Department of Medical Critical Care Medicine, General Hospital of Southern Theatre Command of Peoples Liberation Army, Guangzhou, Guangdong, China

*These authors contributed equally to this work.

ABSTRACT

Sepsis remains a major cause of morbidity and mortality worldwide, yet its prolonged pathophysiological consequences are poorly understood. Here, we employed a murine cecal ligation and puncture (CLP) model to investigate the prolonged impact of sepsis on survival, systemic inflammation, and organ pathology. Adult male C57BL/6 mice underwent CLP or sham surgery and were monitored for 28 days. Survival was recorded daily, while serial assessments of hematology, serum biochemistry, bacterial load, and cytokine levels were performed. Tissue immunofluorescence was used to characterize myeloid-derived suppressor cells (MDSCs), which are potent immunosuppressive cells that inhibit both adaptive and innate immune responses in sepsis, contributing to sepsis-induced immunosuppression. Histopathological analyses were conducted to evaluate structural changes in major organs. CLP mice displayed markedly reduced long-term survival compared with sham controls. Hematological profiling revealed persistent leukocytosis and an inflammatory response, while serum analyses showed sustained elevations in in bilirubin, creatinine, and blood urea nitrogen, reflecting hepatic and renal injury. Bacterial cultures confirmed systemic microbial persistence, and cytokine measurements indicated ongoing inflammatory activity. Tissue immunofluorescence demonstrated the infiltration of MDSCs across multiple organs, consistent with post-sepsis immunosuppression. Histopathological examination revealed widespread, chronic injury in the lungs, liver, kidneys, and spleen, including inflammatory infiltration, tissue degeneration, and architectural disruption. In conclusion, sepsis induces not only acute systemic inflammation but also enduring immune dysregulation and progressive organ damage. These findings highlight the CLP model as a robust platform for studying post-sepsis sequelae and underscore the need for therapeutic strategies that target long-term organ protection and immune restoration.

Key words: sepsis; cecal ligation and puncture; myeloid-derived suppressor cells; immune dysfunction; organ injury.

Correspondence: Zongfang Ren, Department of Critical Care Medicine, the Second Affiliated Hospital of Kunming Medical University, Kunming, No. 374 Dianmian Avenue, Wuhua District, Kunming, Yunnan 650101, China.
E-mail: zfrenkunming@163.com.
Lingling Wang, Department of Medical Critical Care Medicine, General Hospital of Southern Theatre Command of People's Liberation Army, No. 111 Liuhua Road, Guangzhou, Guangdong 510010, China. E-mail: 317542137@qq.com

Contributions: Zongfang Ren, Haoran Tang, study conception and design, funding support; Lingling Wang, methodology; Ning Tang, data curation; Haoran Tang, Chen Liao, data analysis and interpretation; Zongfang Ren, supervision. All authors, writing – original draft, review and editing. All authors read and approved the final manuscript.

Conflict of interest: the authors declare no competing interests and all authors confirm accuracy.

Ethical approval: this study was approved by the Animal Experiment Ethics Review Committee of Kunming Medical University (Approval number: Kmmu20230225).

Data availability: the datasets used and/or analyzed during the current study are available from the corresponding author on reasonable request.

Funding: this work was supported by the grants from the Basic Research Program of the Science and Technology Department of Yunnan Province (No. 202401AY070001-226 to Z. Ren), and Yunnan Science and Technology Department's Plan for cultivating science and technology talents and establishing platforms (No. 202405AC350066 to H. Tang).

Introduction

Sepsis is a life-threatening syndrome characterized by organ dysfunction caused by a dysregulated host response to infection, and it remains a leading cause of mortality in intensive care units.[1-3] In 2016, the American and European Societies of Critical Care Medicine jointly updated the diagnostic criteria for sepsis and septic shock, introducing the Sepsis-3 guidelines.[4] This redefinition shifted the focus from the systemic inflammatory response syndrome (SIRS) to organ dysfunction -either single- or multi-organ failure- as the key determinant of disease severity. While this change increased the clinical relevance of sepsis definitions, it also highlighted the limitations of existing preclinical models. To address these limitations, a consortium of 31 experts from 13 countries proposed the Minimum Quality Threshold in Pre-clinical Sepsis Studies (MQTiPSS) in 2017, providing standardized guidelines to improve the translational value of animal research.[5] These recommendations emphasized the importance of incorporating clinically relevant parameters, including organ dysfunction, supportive care, and longer-term follow-up. Over the past decade, advances in early recognition, antimicrobial therapy, and organ support have markedly reduced early mortality (within the first 72 h). However, an increasing body of evidence reveals that many sepsis "survivors" enter a state of persistent immune dysregulation, characterized by sustained immunosuppression and heightened susceptibility to secondary infections.[6-8] This chronic immunological impairment contributes to elevated late mortality and diminished long-term quality of life. Despite extensive research on sepsis-induced immune dysfunction, the underlying mechanisms of this prolonged immunosuppressive state remain poorly understood, and the long-term immune landscape in survivors is even less well defined.[9] In line with the Sepsis-3 framework and MQTiPSS recommendations, we established a murine sepsis model that more closely reflects the clinical course of human disease. By incorporating antibiotics and fluid resuscitation, this model ensures survival beyond the acute phase, thereby enabling the study of chronic immune alterations rather than solely acute inflammatory responses. The objective of this study was to comprehensively characterize the immune status of sepsis survivors during the chronic phase using this clinically relevant approach. By focusing on prolonged immune dysfunction, we aimed to uncover mechanisms sustaining immunosuppression and contributing to adverse outcomes. Ultimately, these findings may inform the development of targeted interventions to restore immune function and improve survival among patients recovering from sepsis.

Materials and Methods

Ethical approval and animal husbandry

All animal procedures were conducted in accordance with the National Institutes of Health Guidelines for the Care and Use of Laboratory Animals and approved by the Animal Care and Use Committee of Kunming Medical University (Approval number: Kmmu20230225). Fifty male C57BL/6 mice, eight weeks old and weighing 25-30 g, were obtained from Hunan SJA Laboratory Animal Co., Ltd. The animals were maintained in specific pathogen-free (SPF) facilities in transparent polycarbonate cages at a controlled temperature of 22±2°C, relative humidity of 50±10%, and a 12-h light/dark cycle. Standard chow and water were provided *ad libitum*, and all mice were allowed a one-week acclimatization period before experimentation. Due to the regulatory effects of estrogen and progesterone, female mice can attenuate pro-inflammatory signaling pathways such as TLR4–NF-κB and enhance anti-inflammatory responses in sepsis models. Consequently, females are more prone to developing endotoxin tolerance or an immunosuppressive phenotype during the late stage of sepsis; therefore, male mice were selected for this study.[10,11]

Experimental design and group allocation

Before surgery, mice were fasted for 12 h and deprived of water for 4 h. Animals were randomly assigned via computer-generated numbers into three groups: the experimental group (EG, n=6) subjected to cecal ligation and puncture (CLP) to induce sepsis, the sham operated group (CG, n=6) that underwent laparotomy without cecal ligation or puncture, and the healthy control group (HG, n=6) that received no intervention.

CLP procedure

The CLP model was established following previously published protocols.12,13 with minor modifications. Mice were anesthetized with 3% isoflurane and placed supine on a heated surgical platform. The depth of anesthesia was confirmed by the absence of pedal reflex. After shaving and disinfecting the lower abdomen with 75% ethanol, a 1.5-2 cm midline incision was made to expose the peritoneal cavity. The cecum was gently exteriorized and ligated at its midpoint using a 4-0 absorbable suture, ensuring that the ileocecal valve remained unobstructed. Two through-and-through perforations were made with a 21-gauge needle, and a small amount of fecal matter was extruded to ensure patency. The cecum was then returned to the abdominal cavity, and the peritoneum and skin were closed in two layers. Immediately after surgery, animals received subcutaneous isotonic saline (3 mL/100 g body weight) for fluid resuscitation and were kept on a heating pad until full recovery from anesthesia. Sham-operated mice underwent the same surgical exposure without cecal ligation or puncture. Healthy controls received no surgical intervention.

Postoperative care and monitoring

Postoperative management was standardized across groups. Analgesia was provided with a single intradermal injection of buprenorphine (0.05 mg/kg) after recovery from anesthesia. Analgesics were also administered to the healthy control group and the sham-operated group. Environmental parameters were closely monitored, and welfare assessments were conducted every 1-2 h during the first 12 h, then every 6 h for the next 3 days. Observations included locomotor activity, grooming, touch response, and food and water intake.[14,15] The mouse clinical assessment score for sepsis (M-CASS) was used to evaluate disease severity. Antibiotic administration and fluid resuscitation were initiated 8 h after CLP surgery in mice with an M-CASS score >1, a time point at which animals began to exhibit manifestations of severe sepsis. The resuscitation regimen consisted of intraperitoneal administration of imipenem-cilastatin sodium (25 mg/kg) every 12 h, together with supplemental isotonic saline (3 mL/100 g) administered subcutaneously or intraperitoneally for up to 3 days.

Human endpoints and euthanasia

Human endpoints were defined to minimize suffering: i) complete anorexia for 24 h or ≥3 days of reduced intake (<50% of baseline); ii) inability to stand or ingest food/water for 24 h; or iii) moribund state with hypothermia (<37°C) and severe lethargy. Mice meeting these criteria were euthanized by cervical dislocation under light isoflurane anesthesia, performed by trained personnel.

Blood collection and processing

Blood samples were collected from the inferior vena cava at baseline (T0), 24 h (T1), and 72 h (T2) post-CLP under 2% isoflurane anesthesia following disinfection with 75% ethanol. Sham and healthy controls were sampled at matched time points. Samples were processed by blinded personnel and analyzed in triplicate to ensure accuracy.

Hematology and serum biochemistry

Complete blood counts, including white blood cells (WBCs), neutrophils, and lymphocytes, were measured using an automated hematology analyzer (Sysmex, Kobe, Japan). Serum biochemical markers -total bilirubin (TBi), alanine aminotransferase (ALT), aspartate aminotransferase (AST), and creatinine (Crea)- were quantified using enzyme kinetic assays on a Beckman Coulter automatic biochemical analyzer.

Bacterial load determination

To quantify bacterial burden, 0.1 mL of venous blood was serially diluted in sterile saline (1:10, 1:100, 1:1000), and 0.5 mL of each dilution was plated onto blood agar. Plates were incubated at 37°C for 48 h, and colony-forming units (CFUs) were counted on plates containing 30-300 colonies.

Cytokine quantification

Plasma levels of TNF-α, IL-1β, IL-6, and IL-10 were measured using double-antibody sandwich ELISA kits (Nanjing Jiancheng Bioengineering Institute, Nanjing, China) according to manufacturer instructions. Absorbance at 450 nm was recorded using a microplate reader, and concentrations were calculated from standard curves.

Immunofluorescence staining for myeloid-derived suppressor cells (MDSCs)

Spleen, liver, and colon tissues were harvested at designated time points and fixed in 4% paraformaldehyde for 24 h. After cryoprotection in 30% sucrose, tissues were embedded in OCT compound and sectioned at 8 μm. Sections were blocked with 5% bovine serum albumin containing 0.3% Triton X-100 and incubated overnight at 4°C with primary antibodies against CD11b (BioLegend, San Diego, CA, USA; 101201, diluted 1:500) and Gr-1 (Invitrogen, Carlsbad, CA, USA; 14-5931-82, diluted 1:2,000). After washing, sections were incubated with fluorescently labeled secondary antibodies for 1 hour at room temperature and counterstained with DAPI. DAPI was diluted 1:1,000 and stained for 10 min at room temperature. Fluorescence images were acquired using a fluorescence microscope, and MDSC infiltration was quantified as the percentage of positive staining per high-power field. The tissue fluorescence expression was observed and captured using an upright fluorescence microscope (Eclipse C1, Nikon, Tokyo, Japan). Image selection was performed using the imaging system (Nikon DS-U3), and typical images were scanned and saved with a 3D scanner (Pannoramic SCAN, 3DHISTECH, Budapest, Hungary). Fluorescence intensity quantification was then carried out using ImageJ software.

Histopathology

Lung, liver, and colon samples were fixed in 10% neutral-buffered formalin, embedded in paraffin, and sectioned at 4–5 μm thickness. Sections were stained with hematoxylin and eosin and evaluated using established histological scoring systems by observers blinded to group allocation. Liver injury was assessed

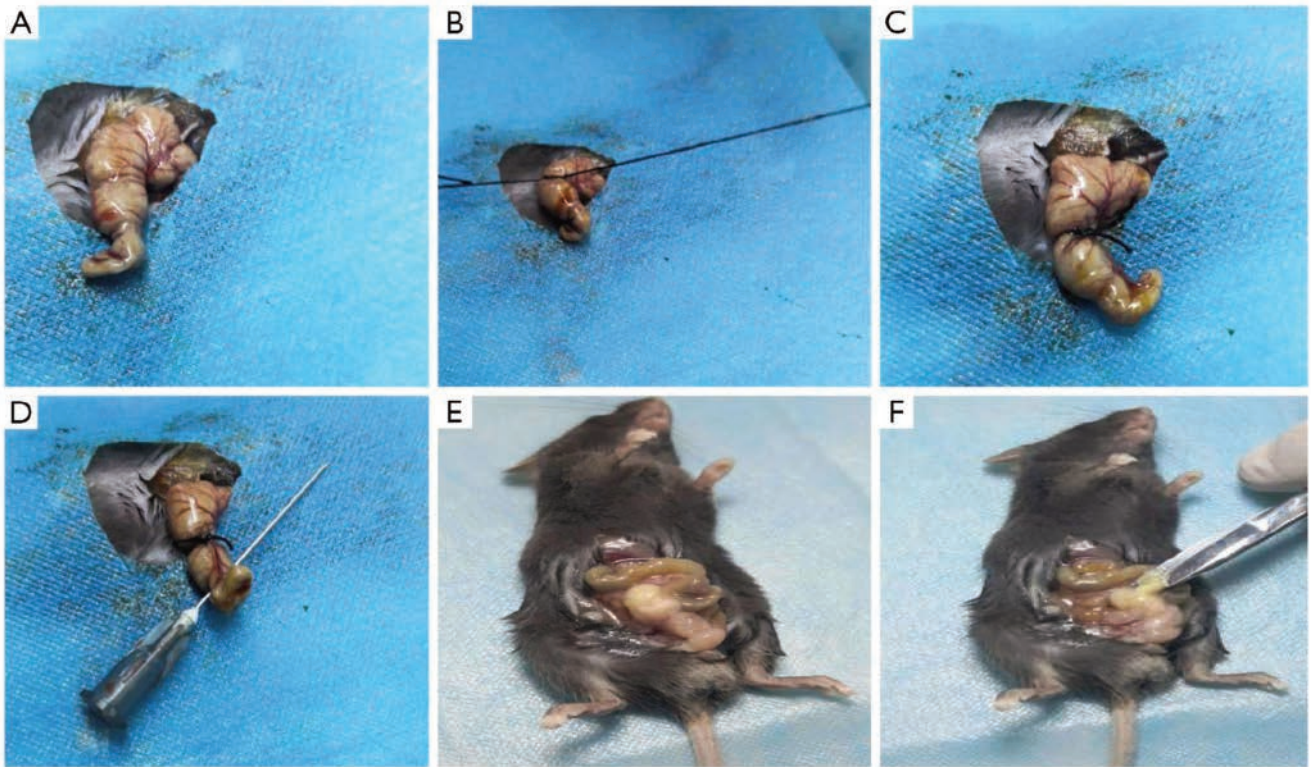

Figure 1. Key procedures of CLP and abdominal abscess formation in septic "survival" mice. **A**) Exposure of the ileocecum and terminal cecum. **B**) Ligation of the distal cecum near the ileocecal valve using 4-0 absorbable suture. **C**) Confirmation of ligation without causing intestinal obstruction. **D**) Cecum puncture with a sterile syringe needle, avoiding vascular injury. **E,F**) In sepsis survivors (15 days post-CLP), an enveloping abscess forms in the ileocecal region, releasing pus upon incision. CLP, cecal ligation and puncture.

using the Chronic Hepatitis Histological Grading/Staging scoring system;{Krishna, 2021 #541}[16] intestinal injury was evaluated using the Ischemia/Reperfusion of the Small Bowel scoring system;[17] and lung injury was evaluated using the A Semi-quantitative Scoring System for Green Histopathological Evaluation of Large Animal Models of Acute Lung Injury.[18]

Statistical analysis

All data were expressed as mean ± SD. Statistical analyses were performed using IBM SPSS Statistics version 24. For normally distributed data, one-way analysis of variance (ANOVA) was applied, followed by Tukey's *post-hoc* test. Non-parametric data were analyzed using the Mann-Whitney U test. A p-value <0.05 was considered statistically significant.

Results

Successful establishment of the sepsis model and clinical features

The CLP procedure was successfully performed, as illustrated in Figure 1 A-D. By two weeks post-surgery, surviving mice developed prominent intra-abdominal abscesses (Figure 1 E-F), confirming the establishment of a chronic infectious focus. Within 6-8 h after CLP, EG mice exhibited classic sepsis-related signs, including crouching, fur ruffling, diarrhea, eye closure, periocular exudates, and shortness of breath. In contrast, sham-operated mice showed only transient reductions in activity and appetite, with recovery by 12 h, and no significant weight changes. Healthy controls remained asymptomatic.

Bacteremia, immune-inflammatory response and organ injury in septic mice

As shown in Table 1, bacterial colonies were consistently detected in the blood of EG mice at baseline (T0), 24 h (T1), and 48 h (T2) after CLP. Sham-operated mice exhibited minimal colony growth at the T0 time point, with no detectable colonies at subsequent time points, which was likely attributable to transient entry of a small number of skin-associated bacteria into the bloodstream during the surgical procedure. Hematological analyses revealed significant increases in leukocytes, neutrophils, and lymphocytes in EG mice across all time points compared with sham and healthy controls (Figure 2 A-C). Sham-operated mice displayed transient elevations at T0 that normalized thereafter, while healthy controls remained within the normal range. TNF-α, IL-1β, IL-6, and IL-10 sharply increased at time T0 in the experimental group, and after treatment, there was a slight decrease at times T1 and T2 (Figure 2 D-G). Although levels fluctuated slightly at T1, they remained significantly higher than in controls, where cytokine concentrations stayed within reference ranges. Biochemical analysis showed significant increases in total bilirubin (TBi) and creatinine (Crea) in EG mice as early as T0, with progressive elevations at T1 and T2 (Figure 2 H-I). In contrast, alanine aminotransferase (ALT) and aspartate aminotransferase (AST) remained within normal limits across all groups (Figure 2 J-K). Sham and healthy control groups-maintained values within reference ranges for all parameters.

Infiltration of MDSCs in the spleen of septic mice

Immunofluorescence staining showed that splenic infiltration of MDSCs ($CD11b^+Gr\text{-}1^+$) was first observed at 48 h after sepsis (Figure 3 A-D). The number of $CD11b^+Gr\text{-}1^+$ cells was markedly increased at 72 h and further elevated at one week post-sepsis (Figure 3 E-L).

MDSCs expression in the liver and colon and organ injury in septic mice

MDSCs infiltration was also observed in the liver and colon. The number of these cells gradually increased over time (Figure 4 A,B). Histological analyses revealed progressive injury in the lung, liver, and intestine of EG mice (Figure 4C). In healthy controls, lung tissues displayed preserved alveolar architecture. At 24 h post-CLP, severe alveolar collapse, pronounced septal thickening, and dense inflammatory cell infiltration were evident. At 48 h, inflammatory infiltration was reduced, although septal thickening persisted. By one-week, partial recovery was observed, with residual alveolar collapse and mild exudation.

In the liver, control tissues exhibited intact hepatic cords and central veins. At 24 h post-CLP, mild sinusoidal dilation and erythrocyte accumulation suggested early congestion. By 48 h, hepatocellular edema, hemorrhage, and structural disorganization became pronounced. At day 7, partial recovery was noted, characterized by reduced inflammatory infiltration, though mild architectural disruption persisted.

In the intestine, control samples displayed intact villi and crypts. At 24 h post-CLP, villus shortening, submucosal edema, and scattered inflammatory infiltrates were observed. At 48 h, villus disorganization, detachment, and extensive inflammatory infiltration were apparent. By one week, partial recovery occurred, with villus restoration and reduced edema, although villus fusion remained evident.

MDSCs produce a range of immunosuppressive and pro-inflammatory mediators, including inducible nitric oxide synthase (iNOS)-derived nitric oxide, reactive oxygen species (ROS), arginase-1, and cytokines such as IL-10. These factors impair cellular function, disrupt tissue homeostasis, and contribute to organ dysfunction during sepsis.

Table 1. Quantitative detection of bacteria in blood.

Group	T_0 logCFU/mL	T_1 logCFU/mL	T_2 logCFU/mL
HG	0.00	0.00	0.00
CG	0.52±0.07	0.00	0.00
EG	1.38±0.1*	0.92±0.12*	1.19±0.04*

*Significant difference between the experimental group and the sham operation group ($p \leq 0.001$). T0, 8 h; T1, 24 h; T2, 72 h; CFU, colony forming units; HG, healthy control group; CG, sham operated group; EG, experimental group.

Discussion

Sepsis is characterized by a profoundly dysregulated immune response, marked by an early phase of excessive immune activation followed by immune tolerance and a prolonged state of inflammation accompanied by immune paralysis. Although most experimental studies have focused on the acute hyperinflammatory phase using conventional CLP or LPS models, accumulating evidence indicates that prolonged immune dysfunction is a key determinant of persistent organ injury and adverse outcomes.[19,20] By incorporating clinically relevant therapeutic interventions and extending the observation window beyond the acute phase, the prolonged sepsis model established in this study more faithfully recapitulates the temporal evolution and immune phenotypes of sepsis, thereby providing a robust framework for dissecting mechanisms of late-stage immune dysregulation and for evaluating

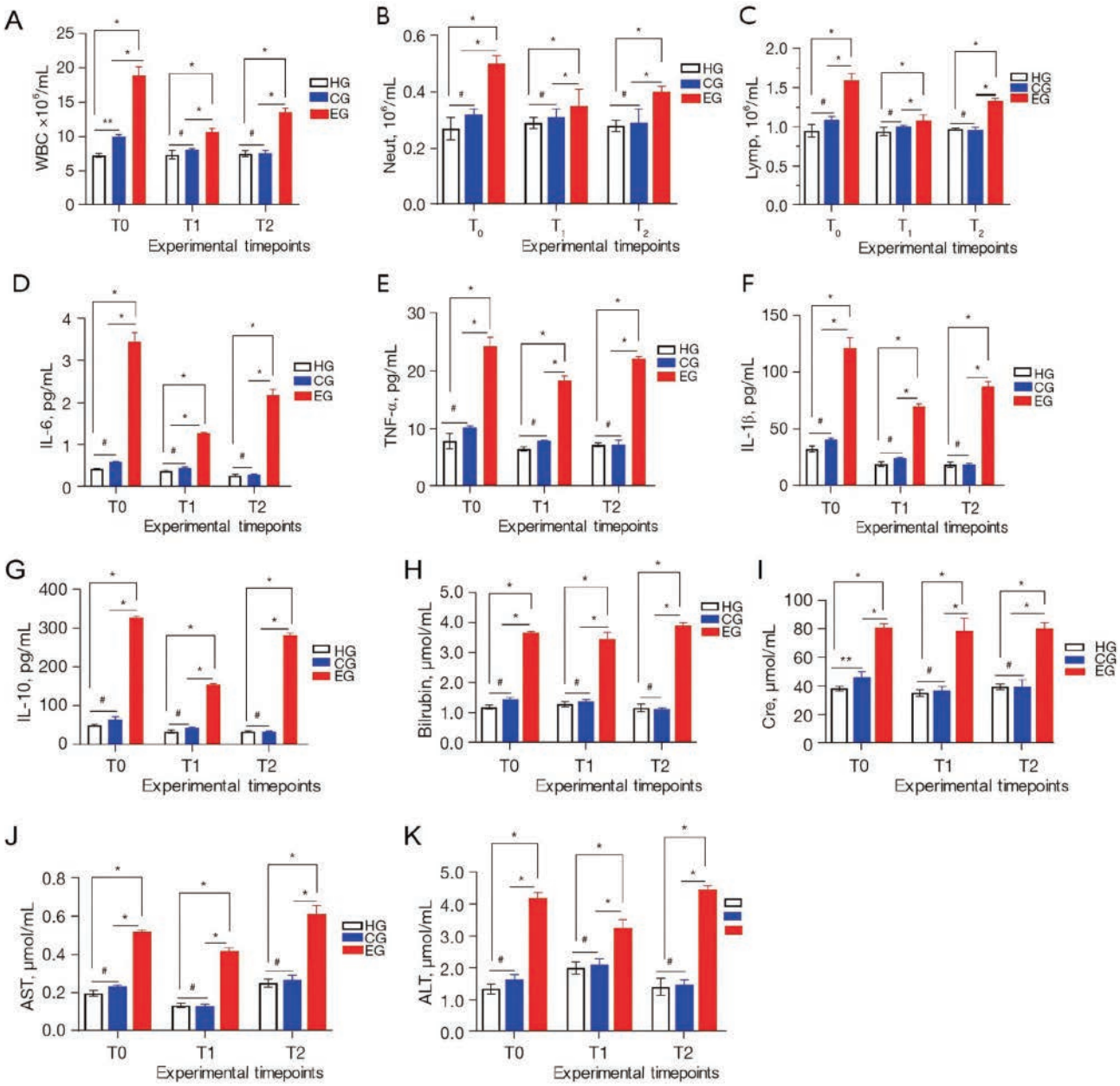

Figure 2. Immune inflammatory response and organ function changes in the healthy group (HG), sham operated group (CG), and experimental group (EG) at T0, T1, and T2. **A**) WBC counts were significantly increased in EG at T1 and T2. **B**) Neutrophil counts were elevated in EG at T1 and T2. **C**) Lymphocyte levels were higher in EG across all time points. **D-F**) Proinflammatory cytokines IL-6, TNF-α and IL-1β levels sharply increased at time T0, and after treatment, there was a slight decrease at times T1 and T2. **G**) Immunosuppressive factor IL-10 concentrations were significantly higher in HG at T1 and T2 compared to CG and EG. **H**) Bilirubin levels increased in HG at T1 and T2. **I**) Creatinine levels were elevated in HG at both time points. J-K) AST and ALT levels were significantly higher in HG at T1 and T2. *$p<0.05$, $^{\#}p>0.05$.

immunomodulatory strategies in a clinically relevant context.

Among preclinical approaches, CLP has emerged as the gold standard for modeling polymicrobial sepsis.[12,21] Unlike lipopolysaccharide (LPS) injection, which induces a rapid but artificial systemic inflammatory response without reflecting the complex hemodynamic and metabolic disturbances of clinical sepsis, CLP better mimics the heterogeneous course of human disease.[22] For this reason, the MQTiPSS guidelines recommend CLP over LPS for translational sepsis research.[23] Incorporating clinically relevant postoperative care, including analgesia, antimicrobial therapy, and fluid resuscitation, is essential for sustaining survival in severe sepsis models and constitutes a key conceptual advance of the present study. Given the polymicrobial nature of intra-abdominal infection and the profound circulatory and microvascular disturbances associated with severe sepsis, such an integrated treatment strategy enables a more faithful recapitulation of the clinical course of the disease, thereby enhancing the translational relevance of the model. As expected, healthy controls maintained stable physiological parameters, while sham-operated mice exhibited only mild and transient leukocytosis and bacteremia, consistent with surgical stress rather than sepsis. By contrast, CLP mice developed progressive bacteremia, elevated pro- and anti-inflammatory cytokines (TNF-α, IL-1β, IL-6, IL-10), and rising biochemical markers of organ injury (total bilirubin and creatinine), all in line with Sepsis-3 criteria for organ dysfunction and systemic infection. A particularly important finding of this study is the early and sustained expansion of MDSCs, characterized as $CD11b^{+}Gr\text{-}1^{+}$ double-positive cells, in both central (spleen) and peripheral (liver, colon) immune compartments. MDSC infiltration was evident by 48 h post-CLP and persisted through later time points, suggesting a central role in mediating post-sepsis immunosuppression. This observation complements and extends previous reports linking MDSCs to immune paralysis in sepsis,[24-26] but our work adds new temporal and spatial detail by mapping their expansion across multiple tissues during the early recovery phase. MDSCs induce immunosuppression in sepsis by inhibiting T cell function, secreting immunosuppressive mediators, and impairing the antigen-presenting capacity of innate immune cells. In malignant tumors, MDSCs similarly suppress antitumor immune responses and are key contributors to tumor progression and metastasis. Our previous studies have also demonstrated a marked expansion of MDSCs in the late stage of sepsis, leading to profound impairment of host immune function. Histopathological findings further demonstrated the dynamic nature of sepsis-induced organ injury, with acute damage to the lungs, liver, and colon evident within 24 h, followed by partial structural recovery by one week. These results highlight the interplay between tissue damage and repair processes and reinforce the systemic character of sepsis pathophysiology.

In conclusion, this study successfully established a clinically relevant murine model of CLP-induced sepsis that fulfills Sepsis-3 diagnostic criteria and incorporates supportive treatments reflective of clinical practice. By enabling survival beyond the acute phase, this model provides a valuable platform for studying long-term immune dysregulation. Post-CLP antibiotic and fluid therapy are critical for ensuring the survival of septic mice and form the foundation for the successful conduct of this study. These interventions also effectively mimic the clinical scenario, representing one of the strengths and advances of this work. Furthermore, we demonstrated that sepsis survivors develop persistent bacteremia, cytokine dysregulation, and sustained multi-organ injury, accompanied by a

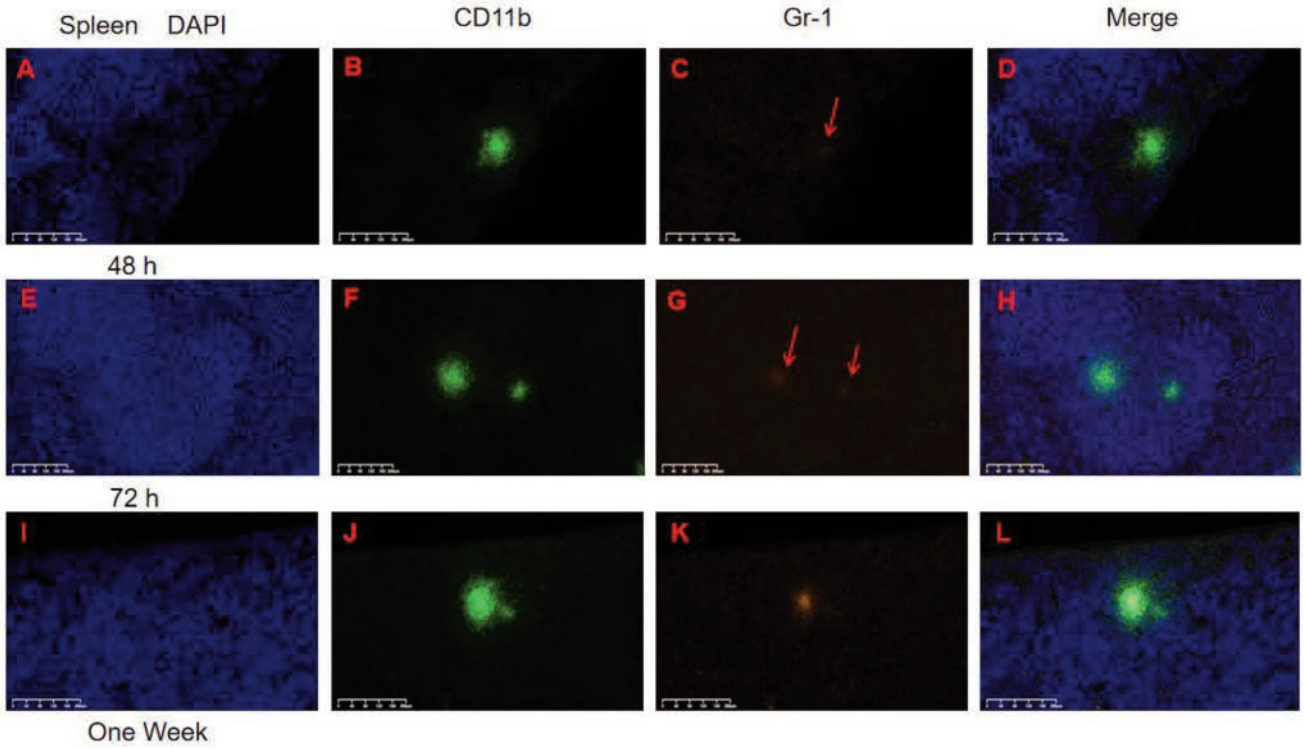

Figure 3. Immunofluorescence analysis of MDSCs in the spleen. **A-D**) At 48 h, sparse $CD11b^{+}$ and $Gr\text{-}1^{+}$ cells were observed (red arrows). **E-H**) At 72 h, both populations increased, with $Gr\text{-}1^{+}$ cells more prominent. **I-L**) At one week, $Gr\text{-}1^{+}$ cells were relatively sparse but clustered in specific regions. Spleen sections were stained with DAPI (blue, nuclei), CD11b (green), and Gr-1 (orange) at 48 h, 72 h, and one week.

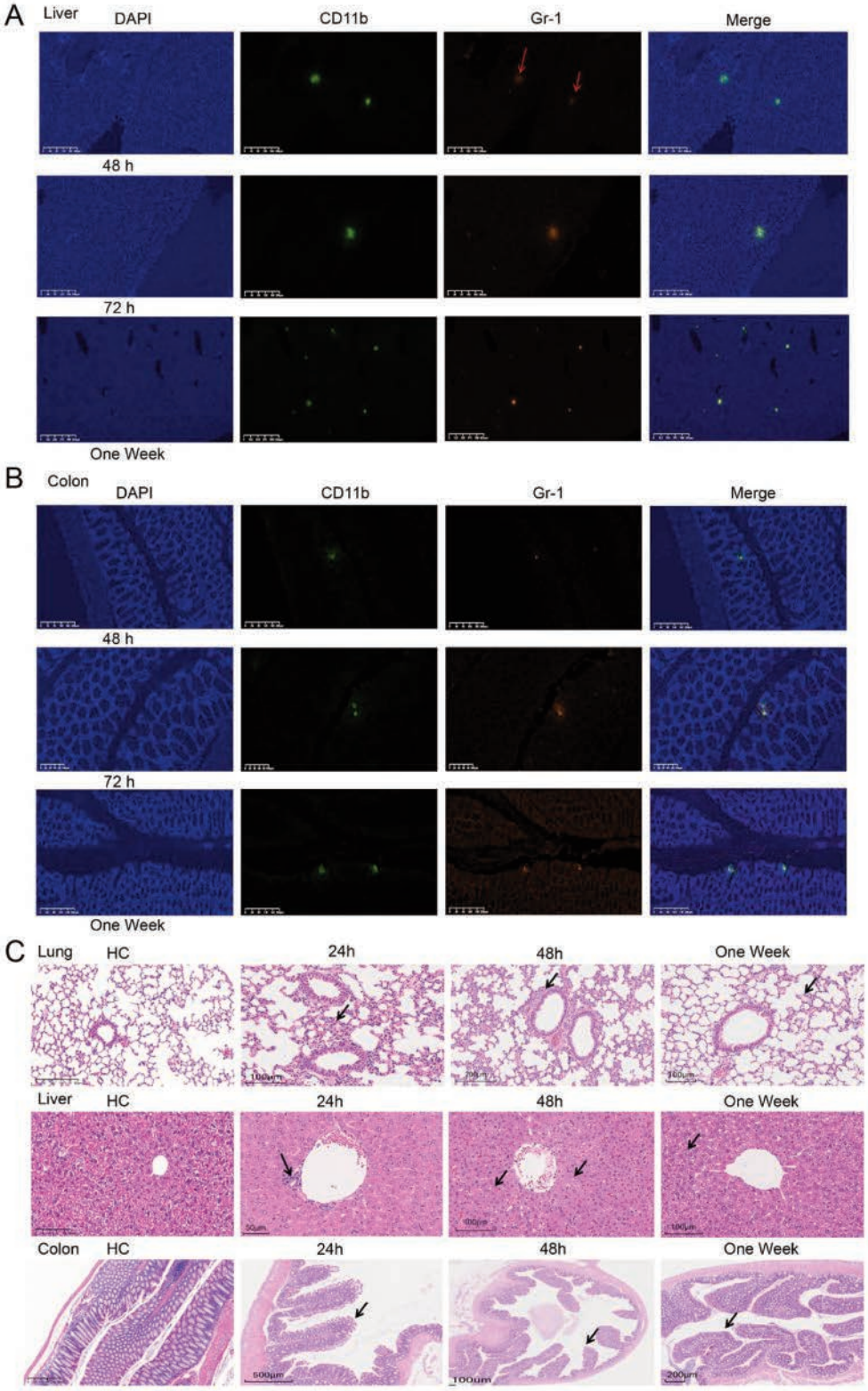

Figure 4. Expression of MDSCs in the liver and colon, and organ damage in major organs (lungs, liver, colon) in septic mice. **A**) Liver sections were stained for DAPI (blue), CD11b (green), and Gr-1 (orange); at 48 h, $CD11b^+$ and $Gr\text{-}1^+$ MDSCs were sparse (red arrows) in liver; at 72 h, both cell populations increased, with $Gr\text{-}1^+$ cells prominently expressed, at one week, $Gr\text{-}1^+$ cells remained relatively sparse but formed clusters in specific areas. **B**) Colon sections were stained with DAPI (blue), CD11b (green), and Gr-1 (orange); at 48 h, $CD11b^+$ and $Gr\text{-}1^+$ MDSCs were sparse; at 72 h, both populations increased, with $Gr\text{-}1^+$ cells more prominent; at one week, MDSCs remained sparse, although clustering was visible in specific regions. **C**) Hematoxylin and eosin staining of tissues at 24 h, 48 h, and one-week post-treatment.

marked expansion and infiltration of MDSCs in both lymphoid and peripheral tissues as early as 48 h after sepsis induction. These findings not only validate the robustness of the model but also implicate MDSCs as central players in post-sepsis immunosuppression. This work establishes a foundation for future mechanistic studies and therapeutic interventions targeting MDSCs and other pathways of immune dysfunction, with the goal of improving outcomes in patients who survive the acute phase of sepsis but remain at risk for chronic critical illness. The present study has a limitation, as tissue immunofluorescence was used for qualitative assessment only, and quantitative fluorescence analysis was not performed. In future studies, we will incorporate systematic quantitative analyses to provide more comprehensive and rigorous evidence.

References

1. Rudd KE, Johnson SC, Agesa KM, Shackelford KA, Tsoi D, Kievlan DR, et al. Global, regional, and national sepsis incidence and mortality, 1990-2017: analysis for the Global Burden of Disease Study. Lancet 2020;395:200-11.
2. Gray A, Sharara F. Global and regional sepsis and infectious syndrome mortality in 2019: a systematic analysis. Lancet Global Healt. 2022;10:S2.
3. Xie J, Wang H, Kang Y, Zhou L, Liu Z, Qin B, et al. The epidemiology of sepsis in Chinese ICUs: a national cross-sectional survey. Crit Care Med. 2020;48:e209-e18.
4. Singer M, Deutschman CS, Seymour CW, Shankar-Hari M, Annane D, Bauer M, et al. The third international consensus definitions for sepsis and septic shock (Sepsis-3). JAMA 2016;315:801-10.
5. Osuchowski MF, Thiemermann C, Remick DG. Sepsis-3 on the block: what does it mean for preclinical sepsis modeling? Shock 2017;47:658-60.
6. Fleischmann-Struzek C, Mellhammar L, Rose N, Cassini A, Rudd KE, Schlattmann P, et al. Incidence and mortality of hospital- and ICU-treated sepsis: results from an updated and expanded systematic review and meta-analysis. Intensive Care Med 2020;46:1552-62.
7. Hawkins RB, Raymond SL, Stortz JA, Horiguchi H, Brakenridge SC, Gardner A, et al. Chronic critical illness and the persistent inflammation, immunosuppression, and catabolism syndrome. Front Immunol 2018;9:1511.
8. Ibarz M, Haas LEM, Ceccato A, Artigas A. The critically ill older patient with sepsis: a narrative review. Ann Intensive Care 2024;14:6.
9. Hotchkiss RS, Monneret G, Payen D. Immunosuppression in sepsis: a novel understanding of the disorder and a new therapeutic approach. Lancet Infect Dis 2013;13:260-8.
10. Sarkar P, Mazgaeen L, Saini S, Gautam N, Paden A, Paton H, et al. Neutrophils are key modulators of sex differences in LPS-induced shock in mice. Blood Vessel Thromb Hemost 2025;2:100104.
11. Bojalil R, Ruiz-Hernandez A, Villanueva-Arias A, Amezcua-Guerra LM, Casarez-Alvarado S, Hernandez-Duenas AM, et al. Two murine models of sepsis: immunopathological differences between the sexes-possible role of TGFbeta1 in female resistance to endotoxemia. Biol Res 2023;56:54.
12. Dejager L, Pinheiro I, Dejonckheere E, Libert C. Cecal ligation and puncture: the gold standard model for polymicrobial sepsis? Trends Microbiol 2011;19:198-208.
13. Rittirsch D, Huber-Lang MS, Flierl MA, Ward PA. Immunodesign of experimental sepsis by cecal ligation and puncture. Nat Protoc 2009;4:31-6.
14. Rinwa P, Eriksson M, Cotgreave I, Backberg M. 3R-Refinement principles: elevating rodent well-being and research quality. Lab Anim Res 2024;40:11.
15. Huet O, Ramsey D, Miljavec S, Jenney A, Aubron C, Aprico A, et al. Ensuring animal welfare while meeting scientific aims using a murine pneumonia model of septic shock. Shock 2013;39:488-94.
16. Krishna M. Histological grading and staging of chronic hepatitis. Clin Liver Dis (Hoboken) 2021;17:222-6.
17. Quaedackers JSLT, Beuk RJ, Bennet L, Charlton A, oude Egbrink MGA, Gunn AJ, et al. An evaluation of methods for grading histologic injury following ischemia/reperfusion of the small bowel. Transplant Proc2000;32:1307-10.
18. Silva IAN, Gvazava N, Bolukbas DA, Stenlo M, Dong J, Hyllen S, et al. A semi-quantitative scoring system for green histopathological evaluation of large animal models of acute lung injury. Bio Protoc 2022;12: e4493.
19. Berikashvili LB, Geize AV, Kornelyuk RA, Plotnikov GP. Immune status in chronic critical illness: a systematic review. Ann Crit Care 2023;1:133-44.
20. Boomer JS, To K, Chang KC, Takasu O, Osborne DF, Walton AH, et al. Immunosuppression in patients who die of sepsis and multiple organ failure. JAMA 2011;306:2594-605.
21. Maier S, Traeger T, Entleutner M, Westerholt A, Kleist B, Huser N, et al. Cecal ligation and puncture versus colon ascendens stent peritonitis: two distinct animal models for polymicrobial sepsis. Shock 2004;21:505-11.
22. Lewis AJ, Rosengart MR. Bench-to-bedside: a translational perspective on murine models of sepsis. Surg Infect (Larchmt) 2018;19:137-41.
23. Libert C, Ayala A, Bauer M, Cavaillon JM, Deutschman C, Frostell C, et al. Part II: minimum quality threshold in preclinical sepsis studies (MQTiPSS) for types of infections and organ dysfunction endpoints. Shock 2019;51:23-32.
24. Arens C, Bajwa SA, Koch C, Siegler BH, Schneck E, Hecker A, et al. Sepsis-induced long-term immune paralysis--results of a descriptive, explorative study. Crit Care 2016;20:93.
25. Bronte V. Myeloid-derived suppressor cells in inflammation: uncovering cell subsets with enhanced immunosuppressive functions. Eur J Immunol 2009;39:2670-2.
26. Gabrilovich DI. Myeloid-derived suppressor cells. Cancer Immunol Res 2017;5:3-8.

Received: 25 October 2025. Accepted: 19 January 2026.

European Journal of Histochemistry 2026; 70:4435
doi:10.4081/ejh.2026.4435